LA-UR -87-2311

CONF-870784--1

Los Alamos National Laboratory is operated by the University of California for the United States Department of Energy under contract W-7405-ENG-36

LA-UR--87-2311

DE87 013147

TITLE: IR LASER EXCITATION IN MOLECULES:
CHAOS AND DIFFUSIVE ENERGY GROWTH

AUTHOR(S): J. R. Ackerhalt
P. W. Milonni

SUBMITTED TO: NATO Workshop on Atomic and Molecular Processes
with Short Intense Laser Pulse
Sherbrooke, Canada
July 19-24, 1987

DISCLAIMER

This report was prepared as an account of work sponsored by an agency of the United States Government. Neither the United States Government nor any agency thereof, nor any of their employees, makes any warranty, express or implied, or assumes any legal liability or responsibility for the accuracy, completeness, or usefulness of any information, apparatus, product, or process disclosed, or represents that its use would not infringe privately owned rights. Reference herein to any specific commercial product, process, or service by trade name, trademark, manufacturer, or otherwise does not necessarily constitute or imply its endorsement, recommendation, or favoring by the United States Government or any agency thereof. The views and opinions of authors expressed herein do not necessarily state or reflect those of the United States Government or any agency thereof.

By acceptance of this article the publisher recognizes that the U S Government retains a nonexclusive royalty-free license to publish or reproduce the published form of this contribution, or to allow others to do so, for U S Government purposes

The Los Alamos National Laboratory requests that the publisher identify this article as work performed under the auspices of the U S Department of Energy

MASTER

Los Alamos National Laboratory
Los Alamos, New Mexico 87545

DISTRIBUTION OF THIS DOCUMENT IS UNLIMITED

IR LASER EXCITATION IN MOLECULES:
CHAOS AND DIFFUSIVE ENERGY GROWTH

Jay R. Ackerhalt and Peter W. Milonni

Theoretical Division T-12
Mail Stop - J569
Los Alamos National Laboratory
Los Alamos, New Mexico 87545

Abstract

After a short review of a generic vibrational model of IR multiple-photon excitation, we generalize the model to include rotations. It is shown that the combination of chaotic dynamics and rotational averaging leads to fluence-dependent absorption which removes the sensitivity of the results to model-dependent parameters. The classical rotation-vibration dynamics observed in this model correlate very well with one's quantum intuition based on a molecule's P, Q and R-branch structure and on the red-shift of the vibrational absorption with excitation. The implication of these results for MPE experiments is discussed.

Introduction

Infrared multiple-photon excitation (MPE) of polyatomic molecules was a major area of research for roughly a decade beginning in 1971 with the work of Isenor and Richardson.[1] Their experiments showed that modest laser powers could easily dissociate a polyatomic molecule. The promise for the future was bond-selective laser photochemistry and laser isotope separation. As this research field grew over the next ten years, it became clear that molecules were not as discriminating with respect to laser wavelength and intensity as was first hoped. By the mid 1980's the field had been nearly abandoned. A few diehards, like ourselves, refused to give up because a solid theoretical explanation of the phenomenon had not yet been found. So here we are today, still talking about MPE.

As the MPE era was winding down in the early eighties, we were aware of the data collection efforts of Judd[2]. He had graphed experimental data on roughly fifty different molecules, all on basically <u>the same fluence-dependent absorption curve</u>, after scaling out the small-signal cross section and excited population fraction. Based on this result we decided that MPE must be a general consequence of the interaction of the laser with the molecule, independent to a certain extent of an individual molecule's idiosycrasies. Therefore we formulated a generic model of MPE incorporating only the essential features of the phenomenon.[3]

Vibrational Model

The Hamiltonian chosen to represent this vibrational model of MPE was

$$\hat{H} = \Delta\, \hat{a}^{\dagger}\hat{a} - \chi\, (\hat{a}^{\dagger}\hat{a})^{2} + \Omega\, (\hat{a}+\hat{a}^{\dagger}) + \sum_{m} (\Delta+\epsilon_{m})\, \hat{b}^{\dagger}_{m}\hat{b}_{m} + \sum_{m} \beta_{m}\, (\hat{a}^{\dagger}\hat{b}+\hat{b}^{\dagger}\hat{a}) \qquad (1)$$

where the terms in order of appearance from left to right represent the anharmonic pump mode (two terms), laser-pump mode coupling, harmonic background modes, and the pump mode-background mode coupling. This form of the Hamiltonian assumes that the laser can be treated classically, the rotating-wave approximation is valid, and the excitation number is conserved. The parameters describing the process are Δ, the frequency detuning of the laser from pump-mode resonance; χ, the pump-mode anharmonicity; Ω, the Rabi frequency; ϵ_{m}, the frequency offset of the mth background mode from the pump mode; and β_{m}, the coupling strength of the mth background mode with the pump mode. Several approximations were made in solving this model based on the general nature of the MPE process; the background modes are equally spaced ($\epsilon_{m} = \Delta_{0} + m\rho^{-1}$, where Δ_{0} is the frequency offset of the zero mode), the background-pump mode coupling is constant ($\beta_{m}=\beta$), and since it takes roughly 30 to 40 photons to dissociate many of the larger molecules like SF_{6}, the dynamics can be solved classically. In addition, the parameters were chosen to be consistent with one's knowledge of molecules: Δ specified for Q-branch excitation, $\chi = 2$ cm^{-1}, $\Omega = .3\ \mathrm{cm}^{-1}$ consistent with roughly 10 $\mathrm{MW/cm}^2$ in SF_6, $\rho = 4/\mathrm{cm}^{-1}$ and $\beta = .2\ \mathrm{cm}^{-1}$.

Using the Hamiltonian (1), making the approximation that the number of background modes is infinite (an approximation justified in the context of radiationless transition theory by Bixon and Jortner[4]), eliminating the background modes, and simplifying the equations using the Poisson summation formula[5], the dynamical equations of motion become

$$\dot{a}(t) = -i(\Delta-\chi)\,a(t) + 2i\chi\,|a(t)|^2 a(t) - i\Omega - (\gamma/2)\,a(t) - \gamma\,s(t) \qquad (2a)$$

$$s(t) = e^{-i\varphi}\,[s(t-\tau_R) + a(t-\tau_R)] \qquad (2b)$$

where $\gamma \equiv 2\pi\beta^2\rho$ is the Fermi Golden Rule rate, $\tau_R \equiv 2\pi\rho$ is the memory recurrence time caused by having an equally-spaced background, and $\varphi \equiv (\Delta + \Delta_0)\,\tau_R$. In Figs. (1a) and (1b) we show the results of integrating Eqs. (2) with $a(0)=0$ and $\varphi=\pi/2$ for $|a(t)|^2$ and the total photons absorbed versus time, respectively. The total absorbed photons have some initial regularity, but after roughly $8\tau_R$ begin an average linear growth whose slope is dependent on the initial choice of φ. In previous calculations for similar parameter regimes the observed dynamics were shown to be chaotic by computing the maximal Lyapunov exponent. In Fig. (2a) we show a Fast Fourier Transform (FFT) of the dynamics shown in Fig. (1a) (Note the characteristic broadband spectrum of chaos.). In Fig. (2b) we show another FFT of the same dynamics as shown in Fig. (1a), except the initial condition has been slightly modified, $a(0)=(.05\sqrt{2})e^{i\pi/4}$. The spectra shown in Figs. (2) are very different considering the rather small change in initial condition. This high degree of spectral sensitivity to initial conditions is a nonrigorous but inexpensive measure of chaotic dynamics, as FFT computations are much faster than the corresponding Lyapunov-exponent calculations. Since the laser pulse envelope is square, the linear absorption of photons reflects a fluence-dependent absorption, consistent with experimental trends. In fact we argued that the chaotic absorption of photons is the bond that links the fluence dependence shown by so many different molecules. However, the sensitivity of the slope to φ was an unsettling feature of this model.

It is interesting to point out that chaotic dynamics and an average linear energy growth in time have been observed in other systems. Casati et al. found this same type of energy growth in the periodically kicked pendulum.[6] Similar results were reported by Leopold and Percival, who considered a classical model of a hydrogen atom in a sinusoidal electric field.[7] Further related work was recently described by van Leeuwan et al., who report excellent agreement between their classical computations and their experiments on the microwave ionization of hydrogen.[8] This research coupled with our own work on MPE illustrates the importance of chaos in these driven systems.

In order to make a real comparison with experiment we decided to couple Maxwell's equations to the molecular medium.[9] As interesting as the results were, we again found a strong sensitivity to φ. Thus it became clear that any treatment of MPE which had any hope of comparing directly with experiment must include the molecule's rotational structure.

Rotational Model

Including rotations at lowest order in a MPE model was previously done by Galbraith, et al.[10] In this case the pump mode was harmonic, and no background modes were included in the model. The resulting chaotic dynamics occurred entirely from the (nonlinear) coupling of the rotation of the molecule with the laser. The rotational dynamics were contained in the dipole coupling term which consisted of the laser in the lab frame and the vibrational dipole moment in the molecular frame. In related work Jones and Percival found that even for constant rotational angular momentum the additional time dependence in the dipole coupling term was sufficient to give a fluence dependent absorption, which was not exhibited by their purely vibrational model.[11]

Following the work of Galbraith, et al., we have included rotations in this quasicontinuum model of MPE. The Hamiltonian (1) becomes

$$\hat{H} = \Delta\, \hat{a}^\dagger \hat{a} - \chi\, (\hat{a}^\dagger \hat{a})^2 + \Omega\, P_3\, (\hat{a}+\hat{a}^\dagger) + \sum_m (\Delta+\epsilon_m)\, \hat{b}^\dagger_m \hat{b}_m + \sum_m \beta_m\, (\hat{a}^\dagger \hat{b} + \hat{b}^\dagger \hat{a})$$

$$+ B_0\, (\hat{J}_1^2 + \hat{J}_2^2) \qquad (3)$$

where the laser-molecule coupling term has been modified to include the direction cosine matrix of the molecule relative to the laser, oriented along the 3-axis in the lab frame. The last term represents the rotation of the molecule about the 1- and 2-axes. This model is simplified in that the nondegenerate pump mode, oriented along the 3-axis in the molecular frame, is treated as a diatomic molecule, so that it has no rotational angular momentum along that direction. The value of B_0 is chosen as 0.1 cm^{-1} in all cases.

The dynamical equations governing this system, making all the same assumptions as was done for Eqs. (2), are

$$\dot{a}(t) = -i(\Delta-\chi)\, a(t) + 2i\chi\, |a(t)|^2 a(t) - i\Omega\, P_3(t) - (\gamma/2)\, a(t) - \gamma\, s(t) \qquad (4a)$$

$$s(t) = e^{-i\varphi}\, [s(t-\tau_R) + a(t-\tau_R)] \qquad (4b)$$

$$\dot{J}_1(t) = \Omega\ P_2(t)\ (a(t)+a^\dagger(t)) \tag{4c}$$

$$\dot{J}_2(t) = -\ \Omega\ P_1(t)\ (a(t)+a^\dagger(t)) \tag{4d}$$

$$\dot{P}_1(t) = -\ 2B_0\ J_2(t)\ P_3(t) \tag{4e}$$

$$\dot{P}_2(t) = 2B_0\ J_1(t)\ P_3(t) \tag{4f}$$

$$\dot{P}_3(t) = -\ 2B_0\ (J_1(t)P_2(t)\ -\ J_2(t)P_1(t)) \tag{4g}$$

where for ease in comparing results from this model with the earlier vibrational model, we have specified $P_3(0) = 1$, $P_2(0) = P_1(0) = J_2(0) = 0$. Therefore, we recover the previous vibrational model for $J_1(0) = 0$ and have a simple rotational model for $J_1(0) \neq 0$. From Eqs. (4) the absorbed rotational and vibrational energy in the molecule are

$$\text{Abs. Rot. Energy} = -\ 2\Omega \int_0^t \dot{P}_3(t')\ \mathrm{Re}(a(t'))\ dt' \tag{5a}$$

$$\text{Abs. Vib. Energy} = -\ 2\Omega \int_0^t P_3(t')\ \mathrm{Im}(a(t'))\ dt'\ . \tag{5b}$$

In Figs. (3a) and (3b) we show the square of the rotational angular momentum and photons absorbed per molecule vs. time, respectively, computed using Eqs. (4) and (5) with $J_1(0) = 6$. All other parameters have been chosen the same as in Figs. (1). Two aspects of these figures should be noted: the regular region shown in Fig. (1b) in the early absorption regime is absent in Fig. (3b), and the rotational absorption to some extent closely parallels the vibrational absorption. We have confirmed that the dynamics is chaotic using an FFT as described above. In Figs. (4) and (5) we show the exact same dynamics as in Figs. (3), but for the P- and R-branches, respectively, i.e., $\Delta = 3.2\ \mathrm{cm}^{-1}$ and $\Delta = 0.8\ \mathrm{cm}^{-1}$. In comparing Figs. (3) through (5) one immediately notices that the overall absorption is sensitive to detuning. In addition, the R-branch rotational absorption curve very closely parallels the corresponding vibrational absorption curve in both shape and number of quantum changes. This is not completely surprising, since in the R-branch $\Delta J=1$, consistent with a one-to-one correspondence between vibrational and rotational absorption of quanta. What is perhaps surprising is that this calculation is completely classical.

In Figs. (3) and (4) one notices that the P-branch ($\Delta J=-1$) curve for J^2 shows an initial decrease, a flat region and an increasing region. This is again entirely consistent with our quantum intuition, since the anharmonicity of the pump mode shifts the absorption feature to the red with increasing vibrational excitation making the rotational dynamics shift from P- to Q- to R-branch absorption. Our quantum intuition also works well in describing the Q-branch results shown in Fig. (3). In all the cases we studied, the correspondence between rotational and vibrational quantum changes was in very good agreement with our expectations from quantum mechanics in both magnitude and direction.

Since the fluence-dependent chaotic absorption for cases where $J_1(0)>0$ showed linear absorption over the entire time interval with no initial regular period, as in Fig. (1), we began a study where the electric field envelope was time-dependent. We chose two profiles to study: one a fairly wide super-Gaussian and the other a moderately narrow Gaussian, both shown in Figs. (6a) and (6b), respectively. The two pulses were chosen to have the same fluence. In Figs. (7) and (8) we show the excitation using the same parameters and format of Fig. (3), but with the excitation due to pulse envelope formats represented by Figs. (6a) and (6b), respectively. A comparison of these figures shows the very strong fluence (rather than intensity) dependence of the absorption. We should mention, however, that the overall absorption is still very sensitive to the exact value of φ.

Completed Results and Conclusions

We concluded our calculations by performing a rotationally averaged calculation of the molecular absorption. For simplicity we used a temperature of 11.74 degrees Kelvin so that the peak of the Boltzmann distribution was at J=6 and the largest J needed for the calculations was J=20. The calculations were performed for various electric field envelopes, values of φ, and detunings. Our overall results showed only a very slight dependence on φ and a strong fluence-dependent chaotic absorption for pulse envelopes of compact support. (We noted some anomalies when we used full-windowed square pulse shapes which have an instantaneous turn-on and -off.)

The global implication of these calculations is that the strong (onsets with the turn-on of the electric field) fluence-dependent absorption in IR MPE is due to chaos originating in the interaction of the laser with the rotating molecule's anharmonic pump mode and the intramolecular transfer of energy to the remainder of the molecule. This fluence-dependent absorption had previously been attributed to simply a large density of states in the molecular quasicontinuum, justifying a rate-equation description of the MPE process. It is interesting that this Hamiltonian system does not require ad hoc homogeneous broadening mechanisms in order to obtain incoherent rate dynamics. The observable effect of this MPE chaos in experiments is a Beer's law absorption of photons, and as many of us already know, this type of absorption was a hallmark of the majority of MPE experiments performed over the last decade. While this is certainly not definitive proof that chaos plays a fundamental role in MPE, it is a completely consistent interpretation of the experimental results.

We would like to acknowledge our previous collaboration with Harold Galbraith.

References

1) N.R. Isenor and M.C. Richardson, Appl. Phys. Lett. 18, 224 (1971);Opt. Commun. 3, 360 (1971).
2) O.P. Judd, J. Chem. Phys. 71, 4515 (1979).
3) J.R. Ackerhalt, H.W. Galbraith and P.W. Milonni, Phys. Rev. Lett. 51, 1259 (1983); J.R. Ackerhalt and P.W. Milonni, Phys. Rev. A34, 1211 (1986).
4) M. Bixon and J. Jortner, J. Chem. Phys. 48, 715 (1968).
5) See, for instance, M.J. Lighthill, Introduction to Fourier Analysis and Generalized Functions (Cambridge University Press, Cambridge, 1970), p. 67.
6) G. Casati, B.V. Chirikov, F.M. Izrailev and J. Ford, Stochastic Behavior in Classical and Quantum Hamiltonian Systems, Vol. 93 of Lecture Notes in Physics, edited by G. Casati and J. Ford (Springer, Berlin, 1979).
7) J.G. Leopold and I.C. Percival, Phys. Rev. Lett. 41, 944 (1978).
8) K.A.H. van Leeuwen, G.v. Oppen, S. Renwick, J.B. Bowlin, P.M. Koch, R.V. Jensen, O. Rath, D. Richards and J.G. Leopold, Phys. Rev. Lett. 55, 2231 (1985).
9) J.R. Ackerhalt and P.W. Milonni, paper THB3 presented at the International Laser Science Conference, Seattle, Oct. 21-24 (1986); presented at the conference on Lasers, Molecules and Methods, Los Alamos, July 7-11 (1986).
10) H.W. Galbraith, J.R. Ackerhalt and P.W. Milonni, J. Chem. Phys. 79, 5345 (1983); in Coherence and Quantum Optics V, edited by L. Mandel and E. Wolf (Plenum Press, 1984), p. 721.
11) D.A. Jones and I.C. Percival, J. Phys. B: At. Mol. Phys. 16, 2981 (1983).

Figure Captions

1) a) Number of quanta in the pump mode vs. time (τ_R), b) Total quanta in the molecule vs. time (τ_R). Parameters given in the text.
2) Logarithmic plot of FFT vs. frequency (cm^{-1}), a) a(0)=0, b) $a(0)=(.05\sqrt{2})e^{i\pi/4}$.
3) a) J^2 vs. time (τ_R), b) Total quanta in the molecule vs. time (τ_R), Q-branch excitation ($\Delta=2.0cm^{-1}$).
4) Same as Fig. (3), but with P-branch excitation ($\Delta=3.2cm^{-1}$).
5) Same as Fig. (3), but with R-branch excitation ($\Delta=0.8cm^{-1}$).
6) Electric field pulse shapes vs. time (τ_R), a) Broad high order super-Gaussian, b) narrow Gaussian.
7) Same as Fig. (3), but with pulse shape shown in Fig. (6a).
8) Same as Fig. (3), but with pulse shape shown in Fig. (6b).

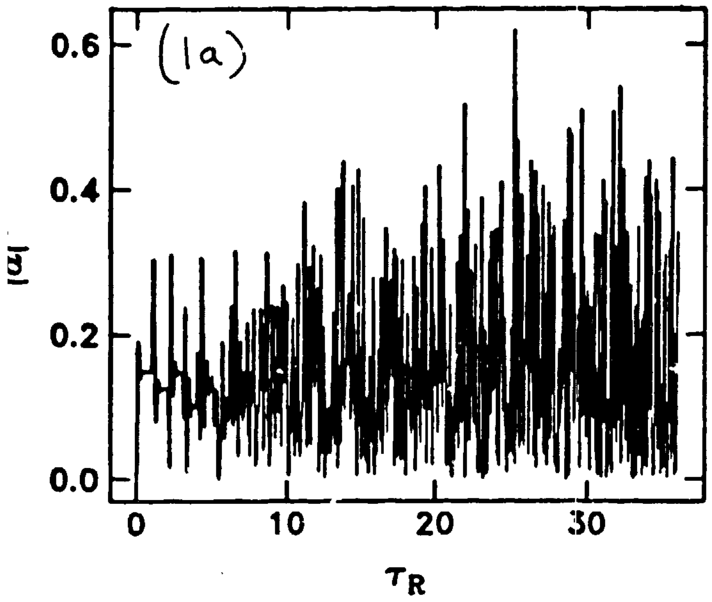
(1a)
|α|
0.6
0.4
0.2
0.0
0
10
20
30
τ_R

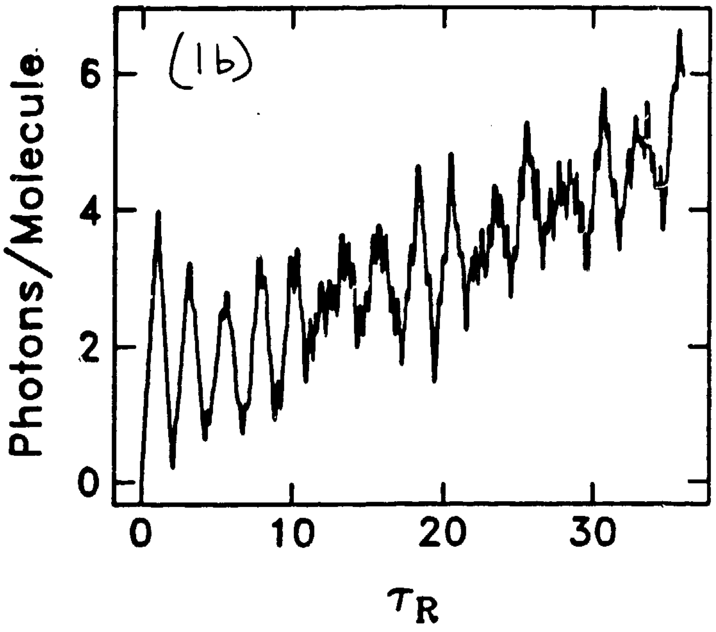
(1b)
Photons/Molecule
6
4
2
0
0
10
20
30
τ_R

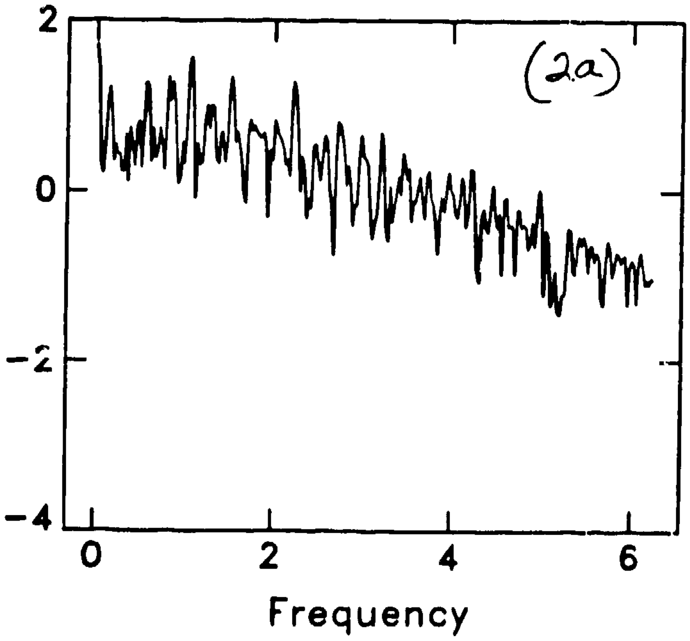
(2a)
2
0
-2
−4
0
2
4
6
Frequency

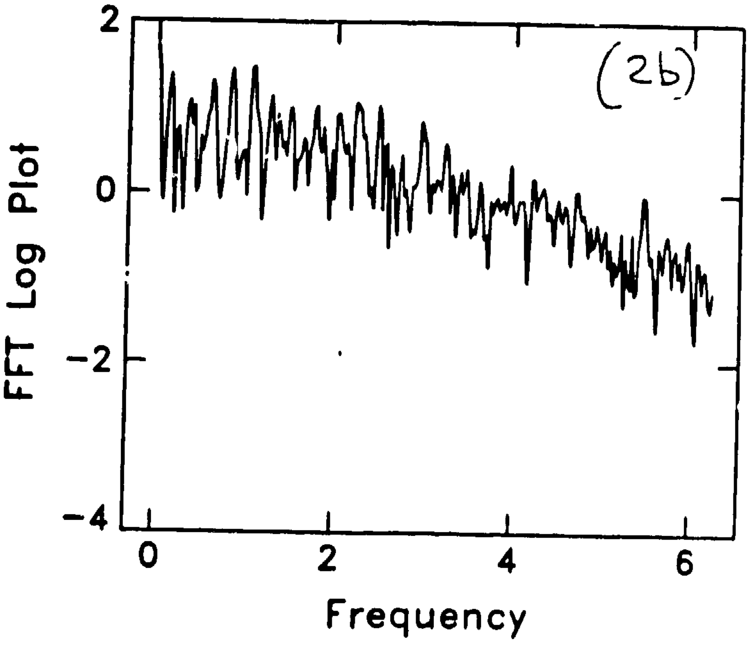
(2b)
FFT Log Plot
2
0
-2
−4
0
2
4
6
Frequency

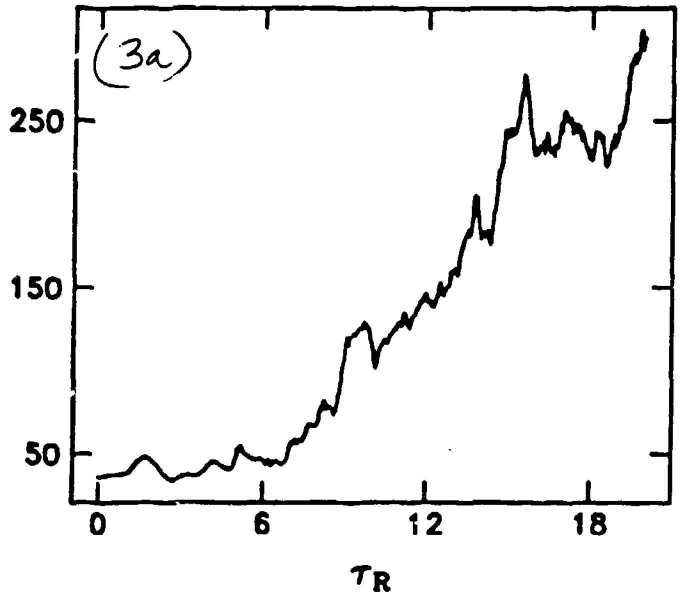
(3a)
250
150
50
0
6
12
18
τ_R

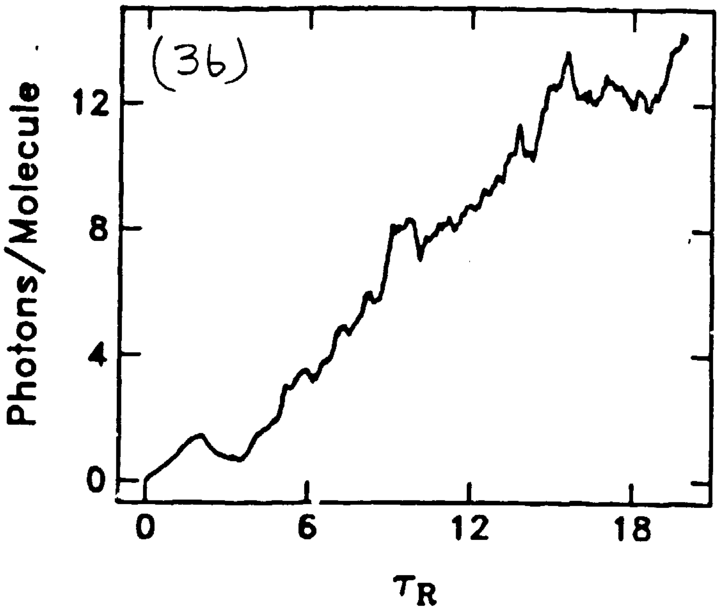
(3b)
Photons/Molecule
12
8
4
0
0
6
12
18
τ_R

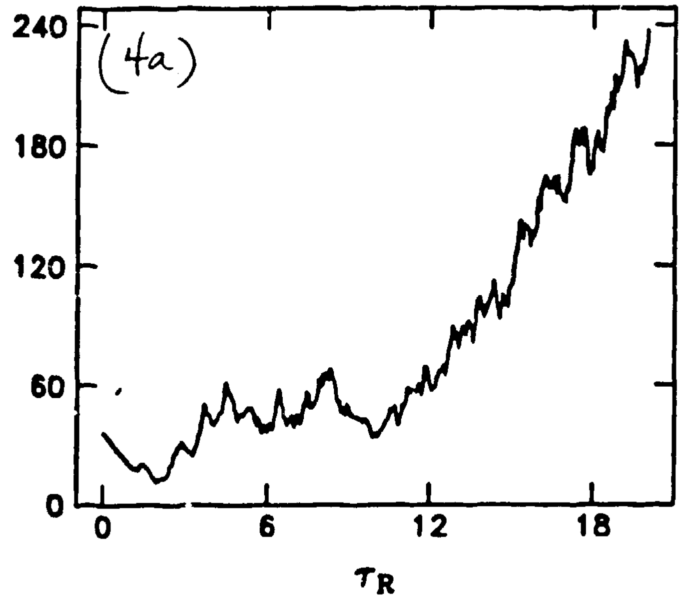
(4a)
240
180
120
60
0
0
6
12
18
τ_R

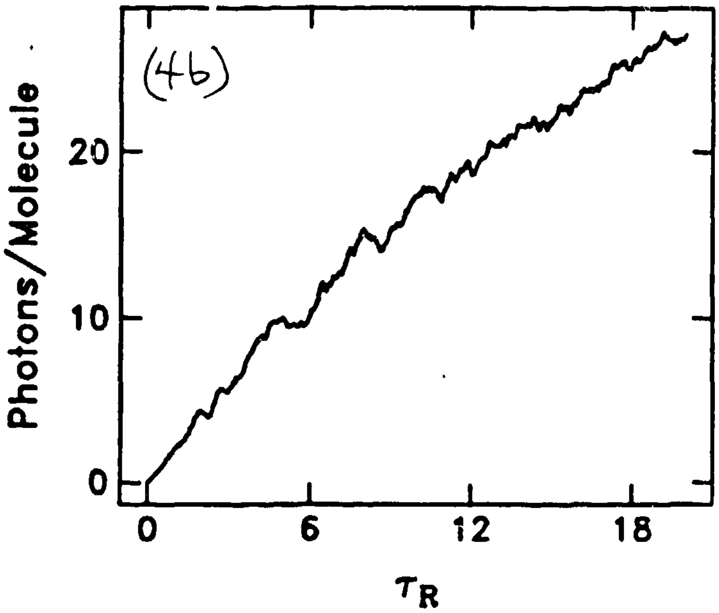
(4b)
Photons/Molecule
20
10
0
0
6
12
18
τ_R

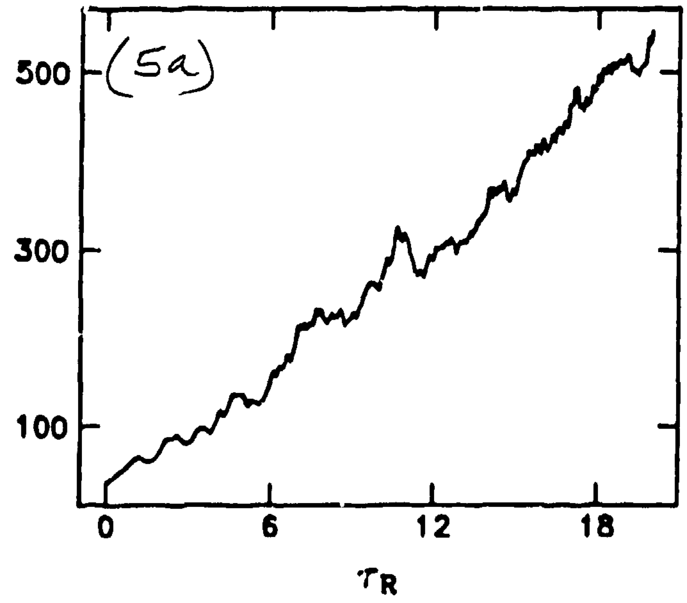
(5a)
500
300
100
0
6
12
18
τ_R

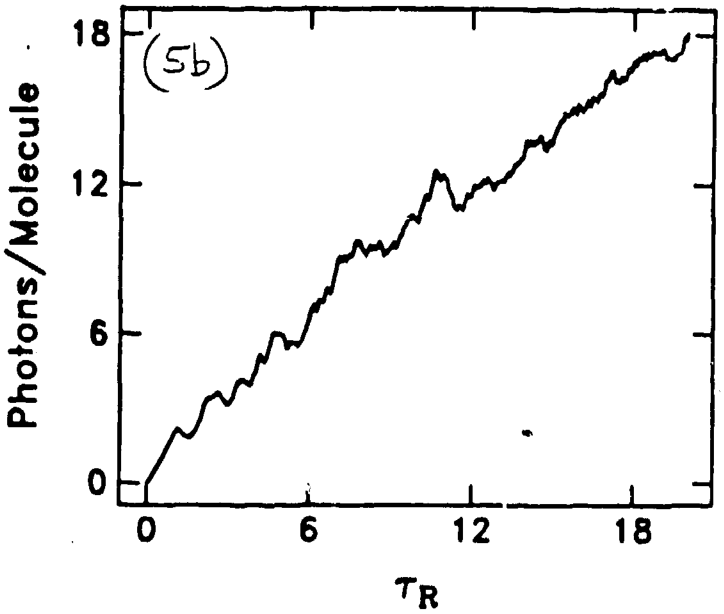
(5b)
Photons/Molecule
18
12
6
0
0
6
12
18
τ_R

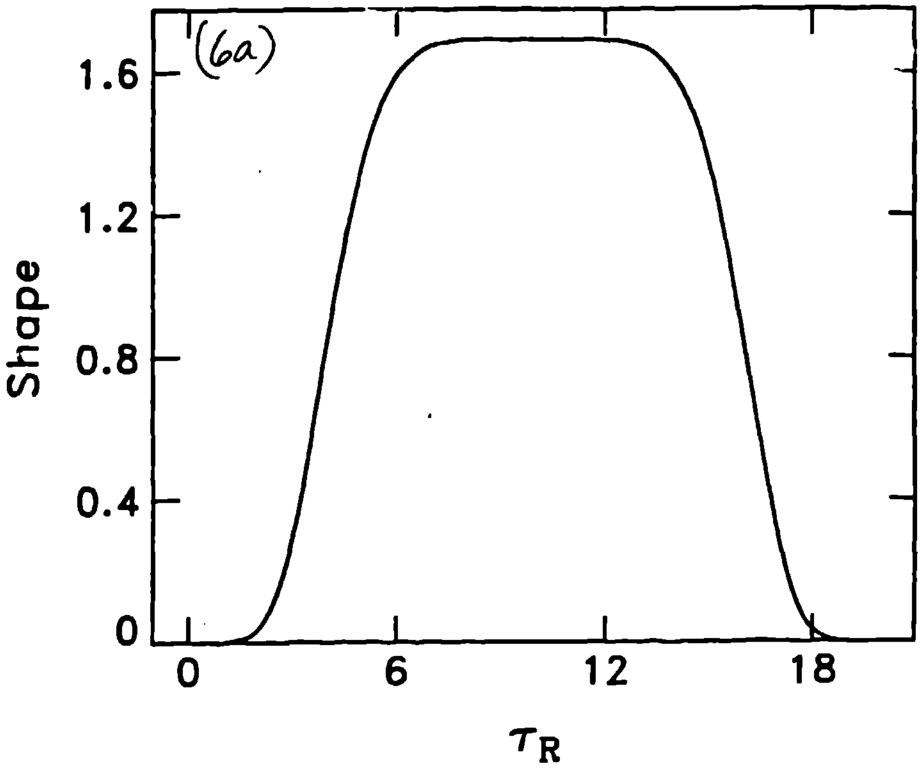

(6a)

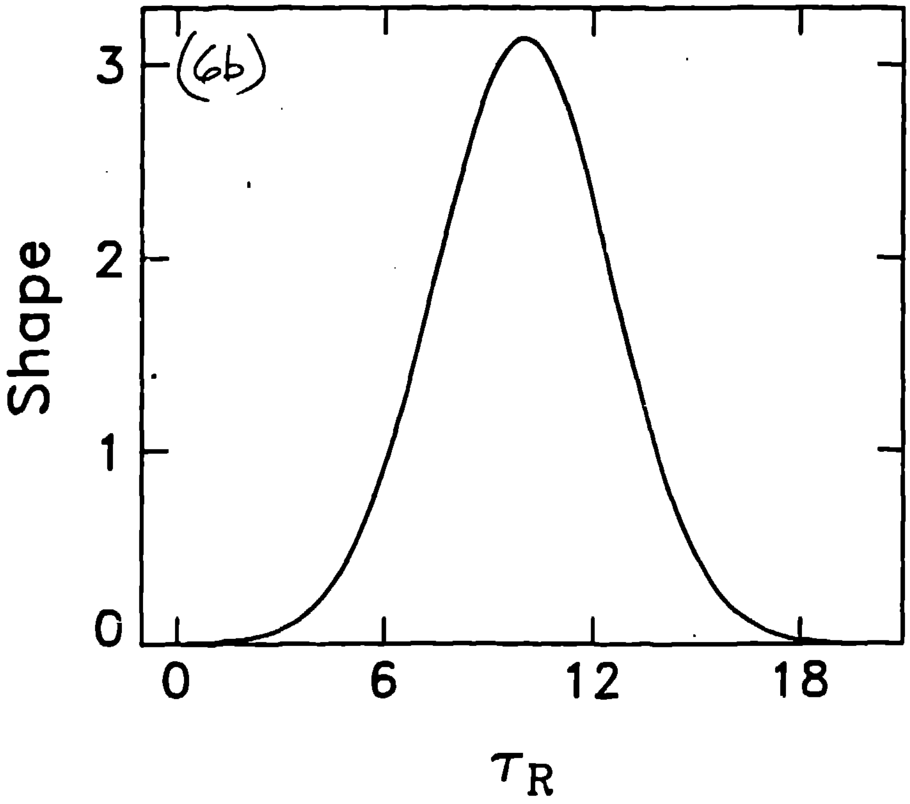

(6b)

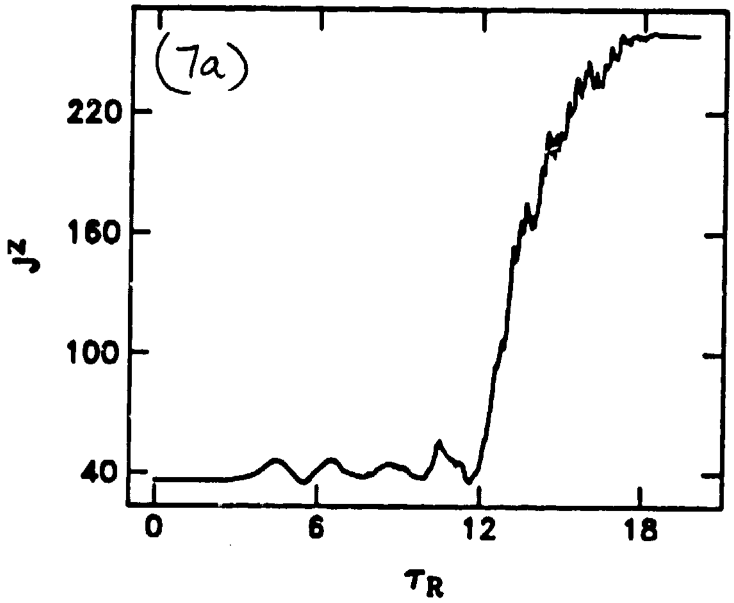
(7a)
J^z
220
160
100
40
0
6
12
18
τ_R

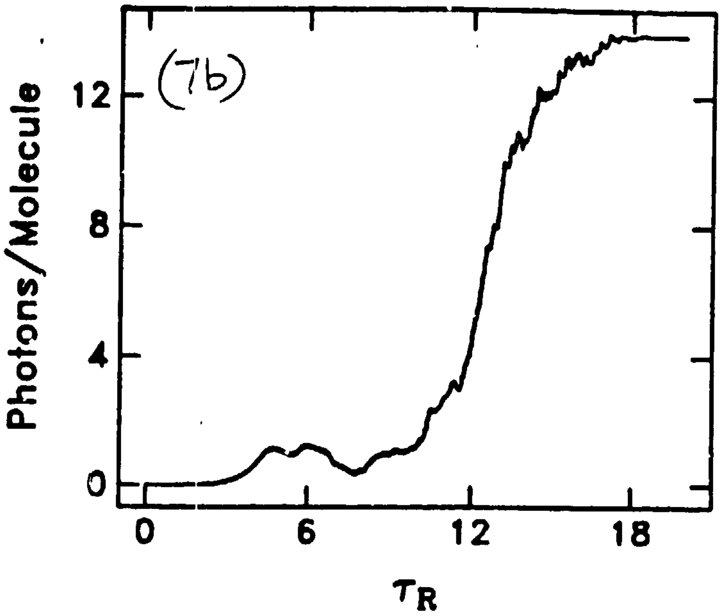
(7b)
Photons/Molecule
12
8
4
0
0
6
12
18
τ_R

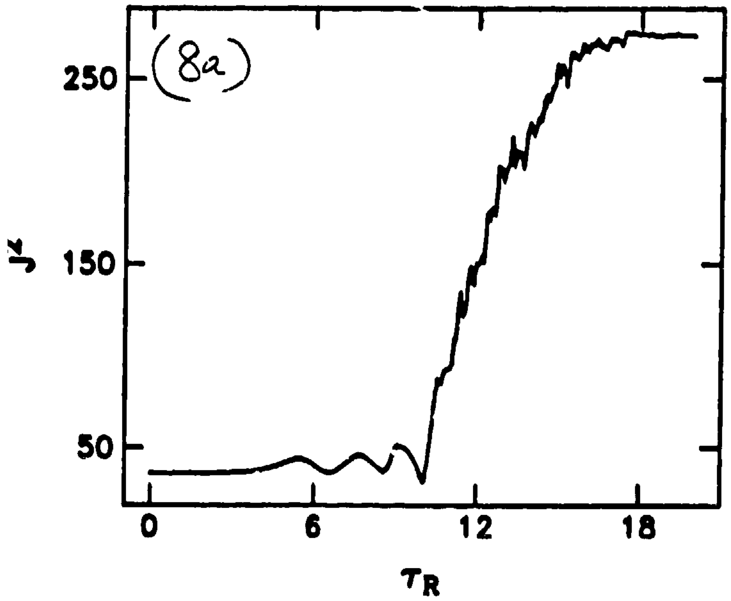
(8a)
J^z
250
150
50
0
6
12
18
τ_R

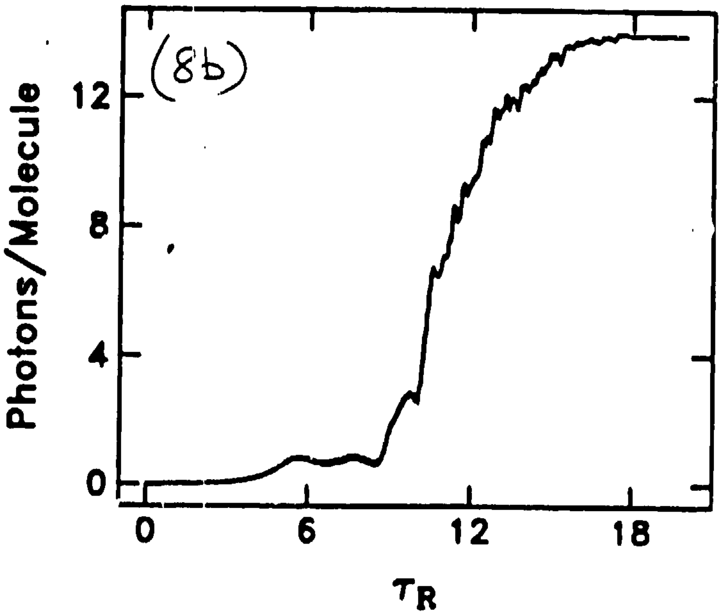
(8b)
Photons/Molecule
12
8
4
0
0
6
12
18
τ_R